A&A 417, L1–L4 (2004)
DOI: 10.1051/0004-6361:20040029

Astronomy & Astrophysics

Hot Very Small dust Grains in NGC 1068 seen in jet induced structures thanks to VLT/NACO adaptive optics⋆

D. Rouan[1], F. Lacombe[1], E. Gendron[1], D. Gratadour[1,3], Y. Clénet[1], A.-M. Lagrange[2], D. Mouillet[2], C. Boisson[5], G. Rousset[3], T. Fusco[3], L. Mugnier[3], M. Séchaud[3], N. Thatte[4], R. Genzel[4], P. Gigan[1], R. Arsenault[1,6], and P. Kern[2]

[1] LESIA – Observatoire de Paris-Meudon, UMR 8109 CNRS, 92195 Meudon, France
[2] LAOG – Observatoire de Grenoble, UMR 5571 CNRS, 38041 Grenoble, France
[3] ONERA – DOTA, 92322 Châtillon, France
[4] MPE, Postfach 1312, 85741 Garching bei München, Germany
[5] LUTH – Observatoire de Paris-Meudon, UMR 8102 CNRS, 92195 Meudon, France
[6] ESO, Karl-Schwarzschild -Str. 2, 85748 Garching bei München, Germany

Received 18 March 2003 / Accepted 15 May 2003

Abstract. We present *K*, *L* and *M* diffraction-limited images of NGC 1068, obtained with NAOS+CONICA at VLT/YEPUN over a 3.5″ × 3.5″ region around the central engine. Hot dust ($T_{\rm col}$ = 550−650 K) is found to be distributed in three main structurally different regions: (a) in the true nucleus, seen as a quasi-spherical, however slightly NS elongated, core of extremely hot dust, *resolved* in *K* and *L* with respective diameters of ≈5 pc and 8.5 pc; (b) along the North–South direction, according to a spiral arm like structure and a southern tongue; (c) as a set of parallel elongated nodules (*wave-like*) on each side, albeit mainly at north, of the jet, at a distance of 50 to 70 pc from the central engine. The IR images reveal several structures also clearly observed on either radio maps, mid-IR or HST UV-visible maps, so that a very precise registration of the respective emissions can be done for the first time from UV to 6 cm. These results do support the current interpretion that source (a) corresponds to emission from dust near sublimation temperature delimiting the walls of the cavity in the central obscuring torus. Structure (b) is thought to be a mixture of hot dust and active star forming regions along a micro spiral structure that could trace the tidal mechanism bringing matter to the central engine. Structure c) which was not known, exhibits too high a temperature for "classical" grains; it is most probably the signature of transiently heated very small dust grains (VSG): *nano-diamonds*, which are resistant and can form in strong UV field or in shocks, are very attractive candidates. The "waves" can be condensations triggered by jet induced shocks, as predicted by recent models. First estimates, based on a simple VSG model and on a detailed radiative transfer model, do agree with those interpretations, both qualitatively and quantitatively.

Key words. galaxies: NGC 1068 – galaxies: Seyfert – galaxies: nuclei – galaxies: dust – galaxies: active – infrared: galaxies – instrumentation: near- and mid-IR – instrumentation: adaptive optics

1. Introduction

At a distance of 14.4 Mpc (70 pc per 1″), NGC 1068 is unique for studying at the scale of a few pc the complex immediate environment of an Active Galactic Nucleus (AGN). Indeed, thanks to muti-wavelength studies, it has been possible in the last decade to identify several distinct features: a structured radio jet issued from a compact source, identified as the central engine (Gallimore et al. 1996), also seen in IR (Thatte et al. 1997); a structured molecular/dusty environment around the central engine of NGC 1068 detected at infrared, millimetric and radio wavelengths (Gallimore et al. 1996; Rouan et al. 1998; Marco & Alloin 2000; Schinnerer et al. 2000; Gratadour et al. 2003); a conical Narrow Line Region (NLR) seen at UV-visible wavelengths and structured in high velocity ionized clouds (Capetti et al. 1995). Studying connections between those structures requires both a good resolution and an excellent registration of the maps at the different wavelengths. Between radio and [visible + near-IR] domains, thermal infrared, can play a unique role. Recently, subarcsecond imaging in the *L* and *M* bands has been reported by Marco & Alloin (2000) and Marco & Brooks (2003) at a resolution of ≈0.2−0.5″. Here we report new results at *K*, *L* and *M* where the spatial resolution and the sensitivity are pushed further thanks to NACO (NAOS + CONICA) the new adaptive optics (AO) system of the VLT, which offers, in addition to an excellent correction of the atmospheric turbulence, the unique capability of thermal infrared imaging at a scale of 0.1″ (Rousset et al. 2002; Lenzen et al. 2002).

Send offprint requests to: D. Rouan,
e-mail: daniel.rouan@obspm.fr

⋆ Based on observations collected at the ESO/Paranal YEPUN telescope, Proposal 70.B-0307(A).

2. Observation and data reduction

The observations were performed using NACO at the Nasmyth focus of YEPUN, during the nights 18−26 of November 2003. The seeing was good (typically 0.6″) and NAOS was servoed on the bright nucleus itself, providing a diffraction-limited correction, as proven for instance by the three rings seen on the PSF in the *M* band. The AutoJitter mode was used, i.e. that at each exposure, the telescope moves according to a random pattern in a 6″ × 6″ box. The pixel scale on CONICA is respectively 0.027″ in the *M* and *L* bands and 0.013″ in the *K* band. On source total integration time was of 640, 800 and 448 s at *K*, *L* and *M*. A PSF reference star, chosen to give equivalent servoing conditions of the AO system, was observed just before and after NGC 1068. Calibration files (flat field at dusk, dark exposures) were acquired as ESO VLT standard data. The *FWHM* of the PSF, estimated from reference stars was respectively 0.061″, 0.105″ and 0.127″ at *K*, *L* and *M*. Applied reduction procedures are fully described in Gratadour, Rouan et al. (2003, in prep.). All images presented here are undeconvolved. The dynamic on the final images ranges from 770 at *L* to 3100 at *M*.

3. Results and discussion

3.1. Registration of radio IR and UV-visible images

We show in Fig. 1, images at *L* and *M*, in a field 3.46″ × 3.46″. The images are diplayed with a power-law scale, so that details of the morphology at all flux levels can be seen. Since several noticeable features are found also on radio, mid-IR and UV-visible images, a very precise registration of all maps can be done. The most conspicuous structure on all images is the bright central extremely compact source, already known at those wavelengths as well as at 10 μm. The bright IR source is most likely the counterpart of the 5 GHz radio source S1 that is unambiguously identified with the central engine because of its spectrum and of the distribution of the maser sources around it (Gallimore et al. 2001). The mid-IR images (Bock et al. 2000) also show a bright central core which obviously marks the location of the same source. The contours of the radio and the mid-IR emissions can thus be superimposed precisely on our IR image, as shown in Figs. 2a,b. A much fainter feature, only present on the M image, is an elongated patch 2.1″ NNE from the core, while another one, seen both at *L* and *M*, is a tongue at 0.69″ NE, with a characteristic shape of a crab claw. Those two features are clearly seen on the images in the UV-visible domain (Capetti et al. 1995), so that it is possible to locate unambiguously – within ≈0.05″ – the IR core on the visible image. Our cross-identification (Fig. 2c) shows that the true nucleus is in fact at the apex of the UV cone, i.e. coincident with the center of polarization vectors in the near-IR and mid-IR (Lumsden et al. 1999): this is the location adopted by Alloin et al. (2001) and more recently by Galliano et al. (2003) who made a very precise astrometric registration of the UV, radio and *K* maps. Two important correlations are also seen in Fig. 2: a) the radio jet is bordered in *L* and *M* by two extended tongues parallel to the jet (the northern being more conspicuous), with enhancements that are tightly

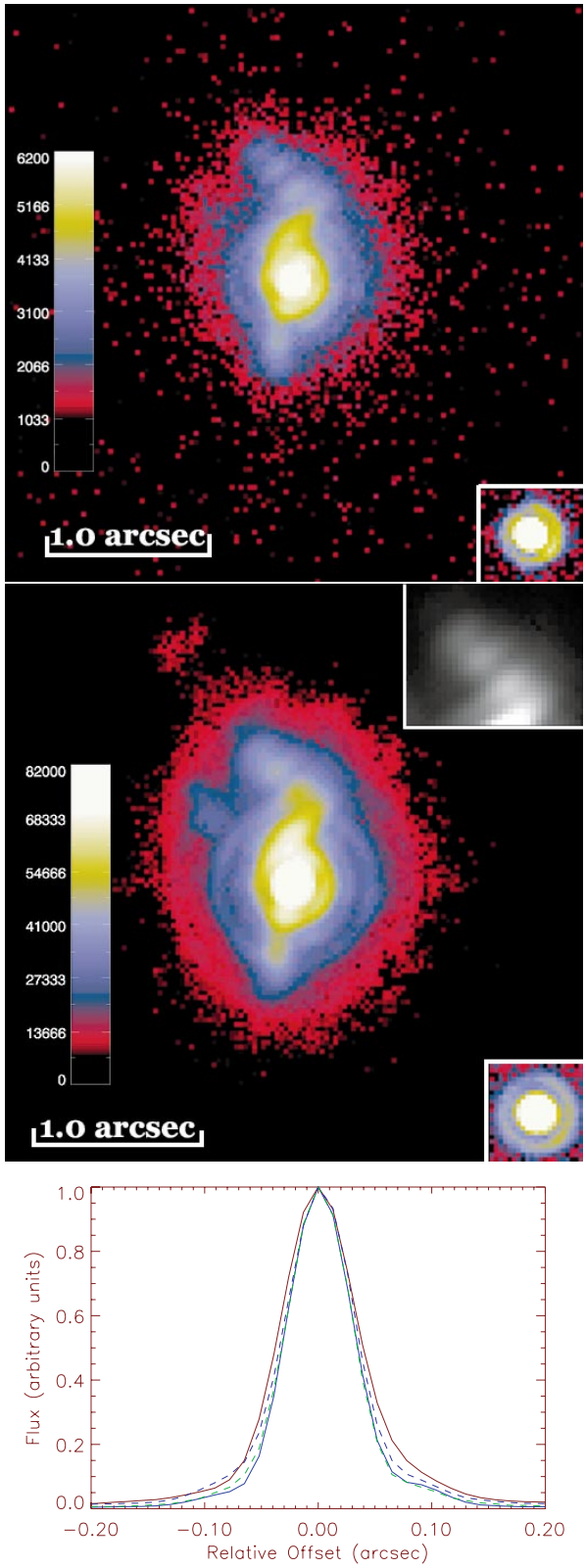

Fig. 1. *Top and middle*: *L* and *M* band false-color images around the core of NGC 1068. The field is limited to 3.46″ × 3.46″. The flux scale, indicated on the color bar, is displayed on a power-law scale ($I^{0.8}$) because of the high dynamic range of the images. The PSF is shown as an inset. *Bottom*: cut of the core at *K*, along NS (solid brown line) and *EW* (dash yellow line) axis; cut of the PSF along NS (solid blue line) and *EW* (dash green line) axis.

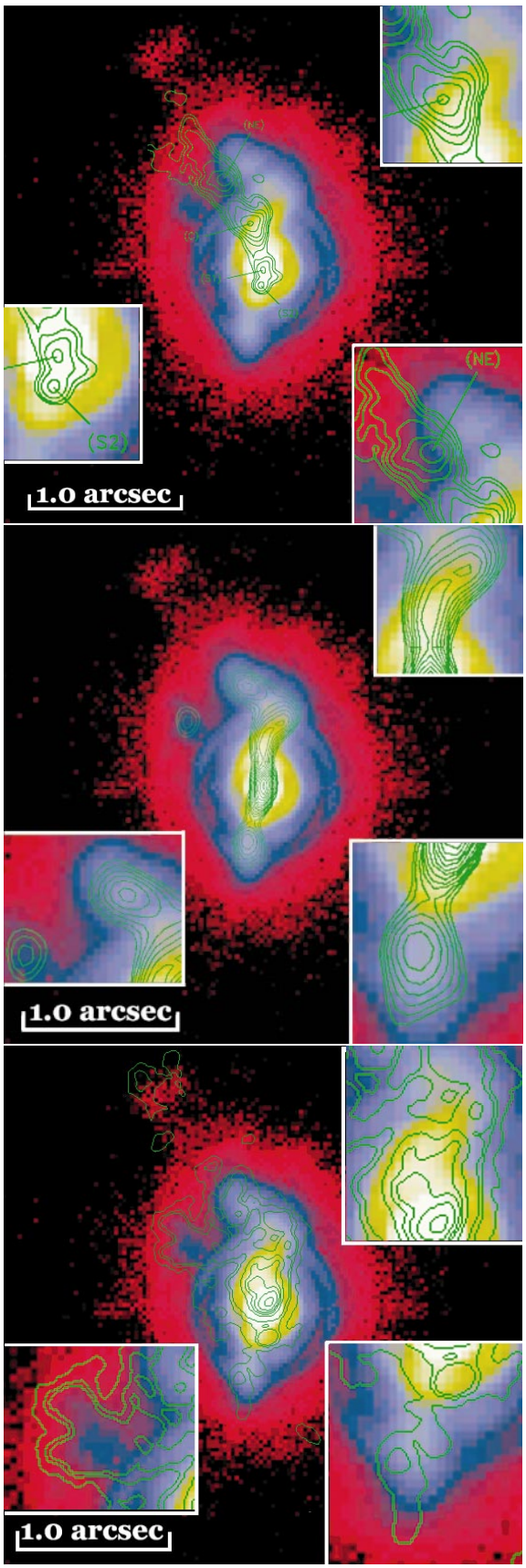

Fig. 2. On our logscale *M* band image are superimposed contours, from top to bottom, of: radio 5 GHz (Gallimore et al. 1996); 12.5 μm (Bock et al. 2000); O III line emission (Capetti et al. 1995). Various insets of magnified regions are also shown.

correlated; b) the 12 μm map does correlate extremely well with the brightest features of the *M* and *L* maps: the NS extension, the NE tongue at the end of the extension and the NE "crab claw".

3.2. The size of the central cavity

The most favoured interpretation (Thatte et al. 1997) is that the core corresponds to the emission from the (UV heated) very hot dust – close to sublimation temperature (1000−1500 K) – delimiting the wall of the central cavity around the accretion disk. This interpretation was recently fully confirmed by CFHT diffraction-limited spectroscopy at a spectral resolution of 220 (Gratadour et al. 2003: GRCLF03), that allowed to derive a color temperature of 950 K and a deredenned one of 1200 K, i.e. close to sublimation temperature of silicates. The new fact brougth by our observations is that the emission is clearly resolved at *K* and at *L*, as revealed by cuts across the core displayed in Fig. 1c. The emission is especially well resolved in the north–south direction, where the measured *FWHM* is .067″ at *K* and .122″ at *L*, i.e. 4.7 pc and 8.5 pc respectively. The *FWHM* at *L* is larger than at *K* because it comes from somewhat cooler, more extended dust. When comparing those results to our model (GRCLF03) – which fairly describes the continuum spectrum in the *K* band at a scale of 0.15″ –, the core size at *K* and *L*, the NS extension, as well as the observed flux ratio are reproduced to within 10%. *The fact that the cavity is resolved is thus a very strong support of the unified AGN scheme.*

3.3. Micro-spiral like structure

Two structures close to the AGN are well defined, especially at *M*. The same structure as depicted by Rouan et al. (1998) of a spiral arm beginning sligthly NE from the core and bending clockwise, up to a point at ≈0.45″ (30 pc) NNW from the center, is observed at all wavelengths. Similarly, a tongue to the south (at a PA of 86°) is clearly observed, with the difference that it does not show a spiral-like structure; it may be obscured by dust from the putative tilted dusty torus (GRCLF03). In both cases, the M/L flux ratio of 1.8 implies a rather high color temperature, larger than 600 K. This ratio is correctly reproduced by thermal emission of grains at 475 K with $Q_{\rm abs} \propto \lambda^{-1.5}$. At this distance (20 pc) from the AGN, the estimated temperature of classical grains with this emissivity is indeed around 475 K, assuming a direct heating by the hard radiation from the accretion disk. In any cases, even an extremely dense stellar cluster cannot heat dust so efficiently. The observed spiral structure is thus more likely dust heated by the central source. It could well traces the innermost stage of nested spirals systems: this type of structure was proposed to produce the required braking torque that brings matter to the center to ultimately feed the "monster" (Shlosman et al. 1989).

4. Hot Very Small Grains in wave-like structures around the jet

This is probably the most striking result we obtained: to the north of the radio jet (see Fig. 2a), four parallel elongated

nodules of ≈0.2″ long each, forming a kind of wave pattern, are observed mainly at *M* and *L*, but also at a much fainter level at *K*. This is especially clear on the inset of Fig. 1a. The first of those structures is in fact the end of the spiral arm described in the previous section. The three others are fairly parallel to it and distributed along a direction which has the same PA as the jet, as if they were delineating the cocoon of the jet. Indeed, the mid-IR images from Bock et al. show an elongated tongue that superimposes very well on the set of "waves" we observe. However, no clues of a sub-structuration were seen on the 12.5 μm deconvolved image. The *K* image, despite the low S/N, indicates that those structures are intrinsically very narrow and probably unresolved in the direction of the jet. It is unlikely that they correspond to classical clouds of gas and/or dust that would be aligned by chance, unless we just see their illuminated front. If the pseudo-periodicity corresponds actually to some physical phenomenon, then the wavelength would be typically of 10 pc. We rather favour the interpretation that this scale is typical of instabilities in the ISM, which developped because of the compression by the jet cocoon. Hydrodynamical models of this interaction indeed predict a nested cylindrical structure with dense clumps on each side of the jet corridor (Steffen et al. 1997, Fig. 2b). The photometry in *L* and *M* reveals unexpectedly high temperatures: for instance, a color temperature of 550 K is derived for the third, well delineated, nodule. At a projected distance of 70 pc, the energy density that is expected at the level of the nodule, assuming that there is no screening of the UV, is $\approx 10^5$ eV. Even under such a large irradiation, the temperature of a *classical* grain would only be 330 K. Redenned free-free emission could be a possible mechanism in a region where the gas is essentially ionized, since the flux density is about twice at *M* than at *L*. However, the corresponding radio or mid-IR emission would be respectively much higher and much lower than observed. Moreover, Bock et al. (2000) have shown that the radio jet cannot be the only heating source, unless the conversion of the shock energy into IR emission is extremely efficient. To reach high temperatures, heating by soft X-rays is a more plausible mechanism that must be explored. Another appealing hypothesis that we favour, is that transiently heated very small grains (VSG) are responsible for this emission. Indeed, this component of the interstellar dust has been invoked years ago (Sellgren 1984) and the prediction that it can contribute very significantly in the near to mid-IR range when the UV field is very strong, is not recent (Désert et al. 1990). Recently, this mechanism was proposed to explain the very red colors observed in ULIRGs (Davies et al. 2002). Nanodiamonds are in fact very good candidates for those VSG in the case of an AGN: (a) they can form very efficiently in a strong UV field or in shocks (Jones & d'Hendecourt 2000); (b) they are not easily destroyed and (c) they can reproduce very well the observed color temperature. Using Jones & d'Hendecourt (2000) heat capacity, we built a model of transient heating, and computed that, for instance, a 0.5 nm diamond absorbing a 6 eV photon and emitting in the IR while cooling, reproduces the observed L/M ratio of nodule #3; a mixture of nanodiamonds from 0.5 to 2 nm receiving photons from 1 to 7.5 eV reproduces the ratio of *L*, *M* and *N* (Bock et al. 2000) fluxes to within 8%. More refined fits will soon be presented (Gratadour et al. in prep.). We predict that several characteristic lines of nanodiamonds should be detectable in this range.

Acknowledgements. We thank the ESO team on Paranal, particularly O. Marco, for the support during observations and the NAOS and CONICA consortia for their superb instruments. Help from C. Catalano was also deeply appreciated.

References

Alloin, D., Galliano, E., Cuby, J. G., et al. 2001, A&A, 369, L33
Bock, J., Neugebauer, G., Matthews, K., et al. 2000, AJ, 120, 2904
Capetti, A., Maccheto, F. D., Axon, D. J., et al. 1995, ApJ, 452, L87
Davies, R. I., Burston, A., & Ward, M. J. 2002, MNRAS, 329, 367
Désert, F.-X., Boulanger, F., & Puget, J.-L. 1990, A&A, 237, 215
Galliano, E., & Alloin, D. 2002, A&A, 393, 43
Galliano, E., Alloin, D., Granato, G. L., & Villar-Martin, M. 2003, A&A, 412, 615
Gallimore, J. F., Baum, S. A., O'Dea, C. P., et al. 1996, ApJ, 462, 740
Gallimore, J. F., Henkel, C., Baum, S. A., et al. 2001, ApJ, 556, 694
Gratadour, D., Rouan, D., Clénet, Y., et al. 2003, A&A, 411, 335
Jones, A. P., & d'Hendecourt, L. 2000, A&A, 355, 1191
Lenzen, R., Hartung, M., Brandner, W., et al. 2003, in Proc. SPIE, 4841, 944
Lumsden, S., Moore, T., Smith, C., et al. 1999, MNRAS, 303, 209
Marco, O., & Alloin, D. 2000, A&A, 353, 465
Marco, O., & Brooks, K. J. 2003, A&A, 398, 101
Rouan, D., Rigaut, F., Alloin, D., et al. 1998, A&A, 339, 687
Rousset, G., Lacombe, F., Puget, P., et al. 2002, in Proc. SPIE, 4839, 140
Schinnerer, E., Eckart, A., Tacconi, L. J., et al. 2000, ApJ, 533, 850
Sellgren, C. 1984, ApJ, 277, 623
Shlosman, I., Frank, J., & Begelman, M. C. 1989, Nature, 338, 45
Steffen, W., Gomez, J. L., Raga, A. C., & Williams, R. J. R. 1997, ApJ, 491, L73
Thatte, N., Quirrenbach, A., Genzel, R., et al. 1997, ApJ, 490, 238